Journal of Organometallic Chemistry, 394 (1990) 515–531
Elsevier Sequoia S.A., Lausanne
JOM 20889

Fluxional behaviour of the clusters $Os_3(\mu\text{-}H)_2(CO)_9(L)$, $L = PMe_2Ph$, PMe_3, P^iPr_3, $P(o\text{-tolyl})_3$ and $PPh(1\text{-naphthyl})_2$. Crystal structure of $Os_3(\mu\text{-}H)_2(CO)_9(P^iPr_3)$ *

Louis J. Farrugia

Department of Chemistry, The University, Glasgow G12 8QQ, Scotland (U.K.)

(Received February 28th, 1990)

Abstract

The variable temperature ^1H, ^{13}C and ^{31}P NMR spectra of the phosphine-substituted clusters $Os_3(\mu\text{-}H)_2(CO)_9(L)$ (**2a**, $L = PMe_2Ph$; **2d**, $L = PMe_3$; **2e**, $L = P^iPr_3$; **2f**, $L = P(o\text{-tolyl})_3$; and **2g**, $L = PPh(1\text{-naphthyl})_2$) are reported. The crystal structure of **2e** shows that the phosphine is substituted at an equatorial site on the $Os(\mu\text{-}H)_2Os$ unit, and in solution this isomer (2_{eq}) is the major species for all derivatives. **2a** and **2d** show minor amounts of the pseudo-axially subsituted isomer (2_{ax}), which exchanges with the major species. No detectable concentrations of 2_{ax} were found with the more bulky phosphines, but for **2a** and **2e** minor amounts of a non-exchanging third isomer were observed, and this was judged to be a species with phosphine substitution at an equatorial site on the $Os(CO)_4$ group. Tripodal rotation of the $Os(CO)_3$ group is found in all derivatives. Clusters **2f** and **2g** show temperature-dependent effects that may be attributed either to a slowed rotation about the Os–P bond or to a slowed inversion of chirality of the propellor configuration of the aryl groups.

Introduction

The study of fluxionality in clusters [1,2] provides information about the mobility of ligands, which in turn may shed light on the mobility of chemisorbed molecules on metal surfaces. Investigations in a series of closely related clusters may provide more quantitative information about the relative importance of steric and electronic factors in determining the exchange activation barriers. For instance Keister and Shapley [3] have studied the exchange between the chemically inequivalent hydrides in the clusters $Os_3(H)(\mu\text{-}H)(CO)_{10}(L)$, and find that there is a clear correlation

---

* Dedicated to Professor F.G.A. Stone on the occasion of his 65th birthday.

0022-328X/90/$03.50

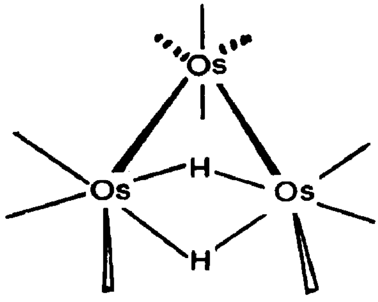

1

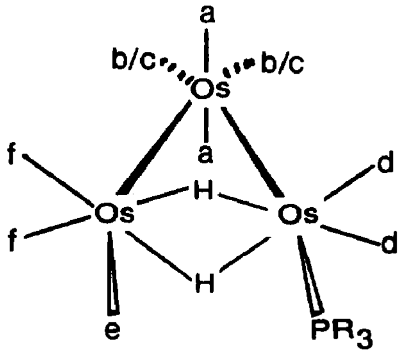

2 (2_{eq})

between an increasing steric bulk of L and a higher activation barrier, and also between an increasing basicity of L and a lower activation barrier.

The fluxional behaviour of the 46-electron unsaturated cluster $Os_3(\mu\text{-}H)_2(CO)_{10}$ (**1**) has been studied in some detail [4–8]. The only CO exchange observed is a slow tripodal exchange in the two $Os(CO)_3$ groups, and analysis of magnetization transfer data [7] and EXSY spectra with various mixing times (t_m) [8] gave exchange rate constants k of 1.08 and 1.21 s^{-1}, respectively, at 300 K. The absence of a kinetic deuterium isotope effect [6] on this CO exchange has been interpreted to indicate that the two (chemically equivalent) hydride ligands are rigid.

We had occasion to prepare ^{13}CO-enriched samples of several phosphine-substituted analogues of **1**, $Os_3(\mu\text{-}H)_2(CO)_9(PR_3)$ (**2**), and describe herein their fluxional behaviour. At the commencement of these studies the only reports on dynamic

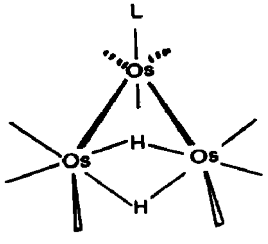

1_{ax}

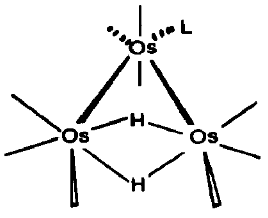

1_{eq}

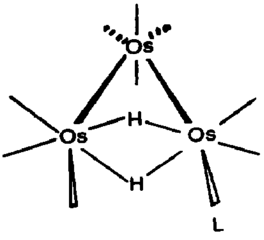

2_{eq}

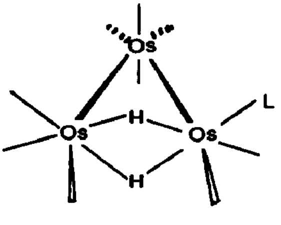

2_{ax}

behaviour of 46-electron derivatives of **1** were brief mentions of a temperature dependence in the ^1H spectrum of **2a** ($R_3 = Me_2Ph$), implying the presence of exchanging isomers [9], and a report stating that the hydride resonance in **2b** (R = Et) showed no change between 213 and 333 K [10]. X-ray analyses on **2c** (R = Ph) [11] and **2a** [12] show that the solid state structures of both are 2_{eq}, while Adams et al. [13] report that the isonitrile derivatives $Os_3(\mu\text{-}H)_2(CO)_9(CNR)$ **3a** (R = Ph) and **3b** (R = ^tBu) have solid state structures 2_{ax} and 2_{eq}, respectively. Clusters **3a** and **3b** exist in solution as both the 2_{eq} and 2_{ax} isomers [13], and very recently Pomeroy et al. [14] have reported the crystal structure of a third isomer, 1_{ax}, of **3b**, and discussed the dynamic behaviour of the various isomers.

Results and discussion

The derivatives $Os_3(\mu\text{-}H)_2(CO)_9(PR_3)$ [**2a**, $R_3 = Me_2Ph$: **2d**, R = Me; and **2e**, R = ^iPr) were prepared by the standard method [9] involving decarbonylation of the decacarbonyl adducts $Os_3(H)(\mu\text{-}H)(CO)_{10}(PR_3)$. Unlike $Os_3(CO)_{12}$, these 48-electron adducts are easily ^{13}CO-enriched by stirring under 1 atm ^{13}CO for ca 1/2 h. The very bulky triarylphosphines $P(o\text{-tolyl})_3$ and $PPh(1\text{-naphthyl})_2$ react only very slowly at ambient temperatures with **1**, and require heating for several hours at 90 ° C. The resulting decacarbonyl adducts are rather unstable under these conditions and readily decarbonylate, giving the nonacarbonyl species **2f** (R = *o*-tolyl) and **2g** ($R_3 = Ph(1\text{-naphthyl})_2$).

All the phosphine derivatives are purple or purplish-brown in colour except for **2e**, which is bluish-green. Although the NMR data (see below) clearly indicate that the principal solution species for **2e** has the structure 2_{eq}, the possibility that the solid state structure was different led us to determine the crystal structure. However, as shown in Fig. 1, the phosphine occupies the same equatorial location on the $Os(\mu\text{-}H)_2Os$ bridge as found for **2a** [12] and **2c** [11]. The structure is thus unre-

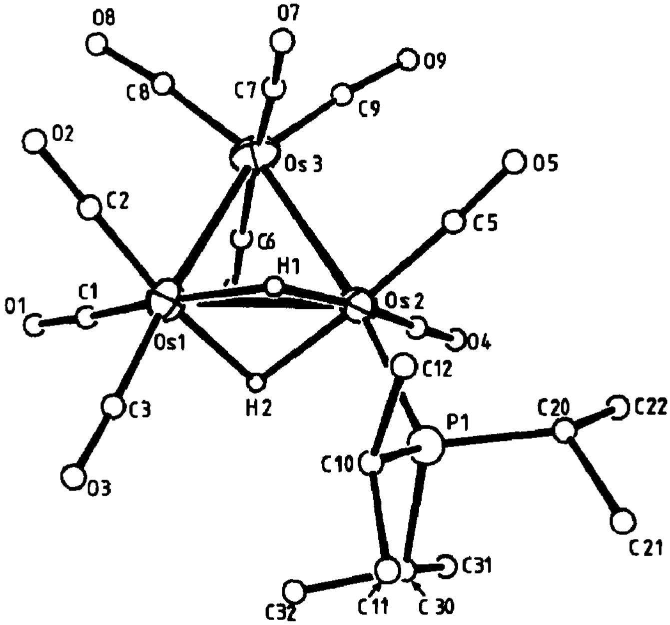

Fig. 1. Molecular structure and atomic labelling scheme for $Os_3(\mu\text{-}H)_2(CO)_9(P^iPr_3)$, **2e**.

Table 1

Final positional parameters (fractional coordinates) with esd's in parentheses, and isotropic thermal parameters (Å^2) (equivalent isotropic parameters U_{eq} for anisotropic atoms) for $Os_3(\mu\text{-}H)_2(CO)_9(P^iPr_3)$ ($U_{eq} = 1/3\Sigma_i\Sigma_j U_{ij} a_i^* a_j^* \boldsymbol{a}_i \cdot \boldsymbol{a}_j$)

	x	y	z	U_{eq}
Os(1)	0.20977(6)	0.11241(8)	0.06853(6)	0.033
Os(2)	0.24418(6)	−0.06040(8)	−0.02652(6)	0.032
Os(3)	0.15722(7)	0.15495(8)	−0.11864(6)	0.044
P(1)	0.3275(4)	−0.2197(5)	0.0778(3)	0.032
O(1)	0.0151(14)	0.1962(17)	0.0361(12)	0.085(6)
O(2)	0.2897(14)	0.3616(18)	0.1127(12)	0.091(6)
O(3)	0.2752(13)	0.0524(16)	0.2711(12)	0.084(6)
O(4)	0.1047(12)	−0.2140(15)	−0.1778(11)	0.065(5)
O(5)	0.3740(15)	−0.0603(18)	−0.1129(13)	0.099(6)
O(6)	−0.0286(13)	0.0344(15)	−0.1574(11)	0.073(5)
O(7)	0.3629(14)	0.2404(17)	−0.0436(13)	0.091(6)
O(8)	0.0726(15)	0.4012(19)	−0.1469(13)	0.100(7)
O(9)	0.1361(16)	0.0963(20)	−0.3079(15)	0.115(7)
C(1)	0.0914(18)	0.1604(22)	0.0478(16)	0.058(7)
C(2)	0.2577(16)	0.2616(21)	0.0953(15)	0.048(6)
C(3)	0.2512(17)	0.0734(20)	0.1917(16)	0.052(7)
C(4)	0.1617(17)	−0.1513(20)	−0.1149(15)	0.048(6)
C(5)	0.3241(17)	−0.0630(21)	−0.0774(15)	0.053(7)
C(6)	0.0411(16)	0.0823(19)	−0.1434(14)	0.039(6)
C(7)	0.2785(18)	0.2049(21)	−0.0775(16)	0.054(7)
C(8)	0.1087(19)	0.3018(25)	−0.1373(17)	0.068(8)
C(9)	0.144(2)	0.125(3)	−0.230(2)	0.09(1)
C(10)	0.4238(14)	−0.1617(17)	0.1903(13)	0.032(5)
C(11)	0.4676(16)	−0.2407(19)	0.2717(14)	0.046(6)
C(12)	0.5030(16)	−0.0952(20)	0.1788(14)	0.050(6)
C(20)	0.3942(16)	−0.3157(20)	0.0346(15)	0.049(6)
C(21)	0.4569(19)	−0.4154(23)	0.0996(17)	0.071(8)
C(22)	0.3364(18)	−0.3649(22)	−0.0616(17)	0.066(8)
C(30)	0.2557(16)	−0.3206(20)	0.1133(14)	0.045(6)
C(31)	0.1765(17)	−0.3839(20)	0.0303(15)	0.052(6)
C(32)	0.2136(16)	−0.2507(19)	0.1656(15)	0.046(6)
H(1)	0.31709	0.04204	0.07040	0.050
H(2)	0.17150	−0.04486	0.03450	0.050

markable and closely resembles that of **2a** and **2c**. Tables 1 and 2 give the atomic coordinates and important bond lengths and angles. The short Os–Os distance of 2.689(1) Å compares very well with that found in **2a** (2.703(1) Å [12]), **2c** (2.683(2) Å [11]) and in **3b** (2.690(1) Å) [13a]), as well as that found in **1** (2.681(1) Å [15]), and implies there is little perturbation of the $Os(\mu\text{-}H)_2Os$ system on ligand substitution. The Os–P distances in **2a**, **2c**, and **2e** (2.347(5) [12], 2.361(2) [11] and 2.384(5) Å respectively) follow the order of increasing steric bulk of the phosphine (Tolman cone angles [16] for PMe_2Ph, PPh_3 and P^iPr_3 are 122°, 145° and 160°, respectively).

Fluxionality of $Os_3(\mu\text{-}H)_2(CO)_9(PMe_2Ph)$, 2a

As previously reported [9], the low-temperature ^1H NMR spectrum of cluster **2a** (Fig. 2) shows an intense doublet in the hydride region at δ −10.85 ($J(P\text{–}H) = 7.9$

Table 2

Selected bond lengths (Å) and bond angles (deg) for the complex $Os_3(\mu\text{-}H)_2(CO)_9(P^iPr_3)$

Os(1)-Os(2)	2.689(1)	Os(1)-Os(3)	2.816(1)
Os(2)-Os(3)	2.822(1)	Os(2)-P(1)	2.384(5)
Os(1)-C(1)	1.81(3)	Os(1)-C(2)	1.79(3)
Os(1)-C(3)	1.86(3)	Os(2)-C(4)	1.74(3)
Os(2)-C(5)	1.81(3)	Os(3)-C(6)	1.86(3)
Os(3)-C(7)	1.79(3)	Os(3)-C(8)	1.77(3)
Os(3)-C(9)	1.77(3)	P(1)-C(10)	1.87(2)
P(1)-C(20)	1.86(3)	P(1)-C(30)	1.87(3)
C-O(carbonyl)	mean 1.21[4]		
Os(2)-Os(1)-Os(3)	61.6(1)	Os(1)-Os(2)-Os(3)	64.4(1)
Os(1)-Os(3)-Os(2)	57.0(1)	Os(1)-Os(2)-P(1)	108.1(2)
Os(3)-Os(2)-P(1)	168.9(2)	P(1)-Os(2)-C(4)	96.1(8)
P(1)-Os(2)-C(5)	92.9(8)	C(1)-Os(1)-C(3)	94.4(11)
C(2)-Os(1)-C(3)	93.4(10)	Os-C-O (mean)	177[2]

Hz) and several weak peaks, which indicate that three isomers are present in solution. The main signal can be attributed to the isomer 2_{eq} observed in the solid state [12]. A doublet resonance at δ −11.14 (J(P–H) = 1.2 Hz), with an intensity ca 1% that of the main resonance, is present in carefully purified, highly crystalline samples of **2a**, and is attributed to an isomer with structure 1_{eq}. The small value of J(P–H) is consistent with this assignment. There is also a sharp doublet at δ 2.35 (J(P–H) = 9.8 Hz) assignable to the methyl protons of this isomer. Any exchange between isomers 1_{eq} and 2_{eq} must involve concerted CO and hydride migration, or

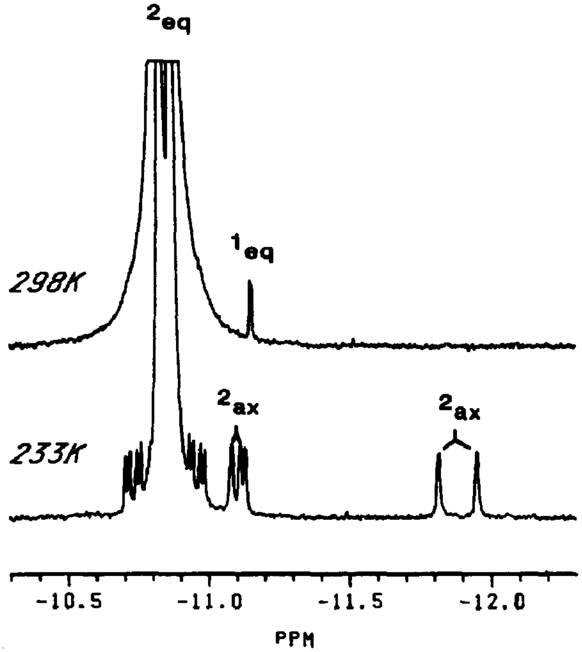

Fig. 2. ^1H NMR spectrum of $Os_3(\mu\text{-}H)_2(CO)_9(PMe_2Ph)$, **2a**, in the hydride region.

phosphine migration, both of which are likely to be high energy processes. The lack of any observable exchange between this minor isomer and the major species provides further circumstantial evidence for this assignment, as does the ^{31}P NMR spectrum, which shows a weak, sharp, resonance at δ −35.7 from 233 to 298 K. Pomeroy et al. [14] have observed that 1_{ax} isomer of **3b** isomerizes slowly (ca 4 days) to the 2_{ax} and 2_{eq} isomers, indicating there are pathways for exchange which are not rapid on the NMR timescale.

In addition to this non-exchanging isomer, there is evidence for another isomer (ca 5%), attributed to 2_{ax}, which does exchange with the major isomer on the NMR timescale. The low-temperature ^{1}H spectrum (Fig. 2) shows two equally intense doublets of doublets at δ −11.10 (J(P–H) = 6.2, J(H–H) = 1.0 Hz) and δ −11.94 (J(P–H) = 27.3, J(H–H) = 1.0 Hz) which may be assigned respectively to the hydrides which are *cis* and *trans* to the PMe_2Ph ligand. On warming, these signals broaden and collapse into the main doublet. Since isomer 2_{ax} does not possess an effective mirror plane, the two methyl groups in the PMe_2Ph ligand are diastereotopic, and at low temperatures appear as two doublets at δ 2.09 (J(P–H) = 10.6 Hz) and δ 2.08 (J(P–H) = 10.5 Hz). The ^{31}P spectrum at low temperatures shows a low intensity signal at δ −17.1 which exchanges with the main signal at δ −8.3. The exchange between isomers 2_{eq} and 2_{ax} may readily be accomplished by a tripodal rotation of the $Os(CO)_2(PR_3)$ group. It has been previously shown that tripodal rotations of $M(CO)_2(PR_3)$ and $M(CO)_3$ groups have similar activation energies [17], and an analogous tripodal rotation of an $Os(CO)_2(CNR)$ group has been proposed to account for the exchange of the 2_{eq} and 2_{ax} isomers of **3b** [14].

The two hydride signals for 2_{ax} show a small mutual coupling, J(H–H) = 1.0 Hz, and similar small couplings have been reported by Pomeroy et al. [14]. Also clearly visible in Fig. 2 are two sets of ^{187}Os satellites about the major signal ($J(^{187}Os–H)$ = 48.5 and 42.3 Hz), due to coupling to the two chemically distinct Os centres. The magnitudes are characteristic of ^{187}Os–μ-hydride couplings at formally unsaturated Os–Os bonds [14,18].

The ^{13}C NMR spectrum of **2a** at 248 K (Fig. 3) shows six sharp resonances, with intensity ratios 2 : 1 : 1 : 2 : 1 : 2, similar to that reported for cluster **2b** [10]. The ^{1}H-coupled spectrum is uniquely consistent with the structure 2_{eq}, and apart from resonances b and c, all signals may be unambiguously assigned on the basis of ^{1}H and ^{31}P couplings and the exchange behaviour. Although it might be anticipated that the carbonyl in the pseudo-*trans* relationship to the phosphine (either b or c) would show ^{31}P coupling (as seen for example in $Os_3(H)(\mu\text{-}H)(CO)_{10}(PMe_2Ph)$ [3]), neither signal has any detectable ^{31}P coupling, nor indeed do the corresponding signals in any of the other derivatives we have studied. The relative assignments of b and c are thus unclear. In $Os_3(CO)_{10}(PMe_2Ph)_2$ we note that there is no such detectable long-range ^{31}P–^{13}C coupling [19]. The ^{1}H-coupled spectrum shows second-order effects on resonances d and f (which are the X part of an AA′MX or AA′X spin system, respectively) due to a non-zero magnitude of J(H–H). Simulations indicate a value of ca 2 Hz for this coupling.

When the solution is warmed to 298 K, all signals show exchange broadening, particularly resonances a, d and e. EXSY spectra recorded at various temperature between 266 and 298 K, with mixing times (t_m) of either 0.5 or 1.0 s, show cross peaks between resonances e and f, indicating a *direct* exchange between these carbonyls [20]. This is consistent with their assignment as the three CO's in the

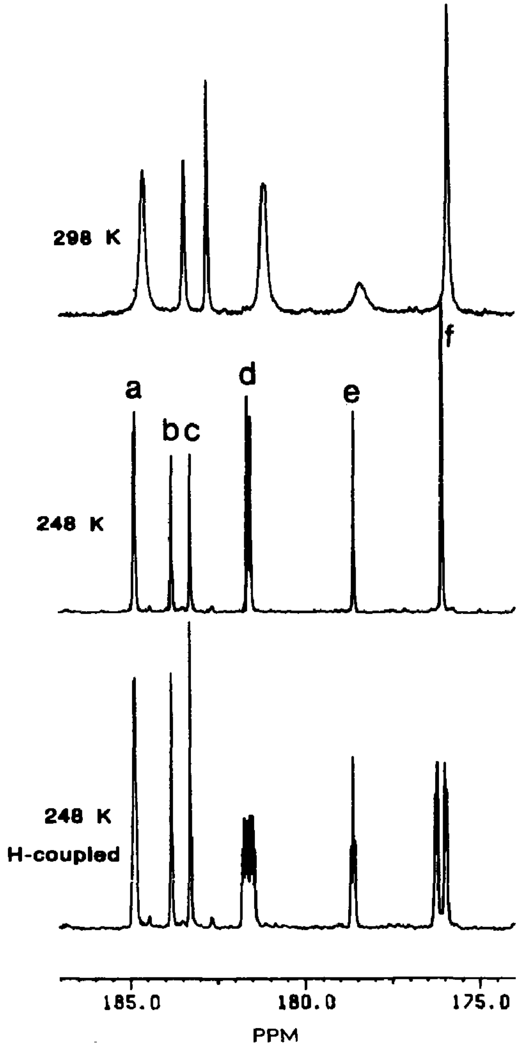

Fig. 3. ^{13}C NMR spectra of $Os_3(\mu\text{-}H)_2(CO)_9(PMe_2Ph)$, **2a**, in the carbonyl region.

$Os(CO)_3$ group, and an *approximate* value of $\Delta G^{\ddagger}_{273} = 70.3(\pm 1.1)$ kJ mol^{-1} was obtained for the degenerate tripodal exchange, using the method of Abel et al. [21]. The analysis is only approximate because there is also a non-degenerate exchange between isomers 2_{eq} and 2_{ax} which also contributes to the line broadening. Resonances a and d are broadened more than b and c, probably because the former pair are involved in a 1- to 2-site exchange in going from 2_{eq} to 2_{ax}, while b and c are only involved in 1- to 1-site exchange.

*Fluxionality of $Os_3(\mu\text{-}H)_2(CO)_9(PMe_3)$, **2d***

The NMR spectra of **2d** show no evidence for an isomer 1_{eq}, but are otherwise quite similar to those of **2a**. The proportion of the isomer 2_{ax} present in solution (ca 17%) is substantially higher. The ^{31}P spectrum at 234 K shows a major singlet at δ -15.1, and a weaker singlet at δ -22.5. These resonances are substantially broadened at 298 K. The ^{1}H spectrum at 234 K in the hydride region shows a major doublet at δ −11.00 (J(P–H) = 8.1 Hz), and two lower intensity signals at δ −11.2 (J(P–H) = 6.3 Hz) and δ −11.69 (J(P–H) = 25.9 Hz). Signals are also observed for the methyl groups at δ 1.95 (major, J(P–H) = 10.2 Hz) and δ 1.80 (minor, J(P–H) = 10.8 Hz), and both sets of hydride and methyl resonances are coalesced at 298 K. The variable-temperature ^{13}C spectrum is qualitatively very similar to that of **2a**, although all resonances are broader at 298 K, indicating slightly faster exchange. Due to the complexity of the fluxional processes, involving both degenerate and non-degenerate exchange, and the relatively low abundance of the minor isomer no quantitative analysis was undertaken.

Fluxionality of $Os_3(\mu\text{-}H)_2(CO)_9(P^iPr_3)$ *(**2e**)*

Both clusters **2a** and **2d**, with the sterically undemanding phosphines PMe_2Ph and PMe_3 (Tolman cone angles [16] 122° and 118°, respectively), have measurable concentrations of the isomer 2_{ax}. The pseudo-axial site is evidently more sterically congested than the equatorial site. This is borne out by the observation [14] that for **3b**, which contains the sterically undemanding ligand CN^tBu, isomer 2_{ax} is preferred to isomer 2_{eq} in solution, even through it is the 2_{eq} isomer which crystallizes out [13]. For the derivative **2e** with the large phosphine P^iPr_3 (cone angle 160° [16]), we find no evidence for a 2_{ax} isomer. There are, however, low-intensity signals attributable to a 1_{eq} isomer, with resonances at δ −11.20 (J(P–H) = 7.0 Hz) in the ^{1}H NMR, and δ 42.8 in the ^{31}P NMR. The main ^{31}P signal at δ 55.9 is invariant from 234 to 298 K, as is the ^{1}H NMR spectrum in the hydride region, which shows a doublet at δ −10.92 (J(P–H) = 6.6).

The ^{13}C spectrum of **2e** is very similar to the low-temperature spectrum of **2a** (see Fig. 3), but with less line broadening at higher temperatures. The ^{13}C{^{1}H} EXSY spectrum (Fig. 4) shows a slow exchange between resonances e and f, and has been analysed by the method of Abel et al. [21] yielding a value of $\Delta G^{\ddagger}_{298} = 69.6(\pm 0.9)$ kJ mol^{-1} for the degenerate tripodal rotation. No other CO exchange processes are seen.

The ^{13}C spectrum at 248 K is of sufficiently high quality to show satellites due to ^{187}Os–^{13}C coupling (see Experimental Section). Of particular interest are the values of the coupling constants to resonances a and b, the axial CO and one of the equatorial CO's of the $Os(CO)_4$ group, which have values of 92 and 116 Hz, respectively. In the parent cluster **1**, the carbonyls in the $Os(CO)_4$ group resonate at ~ δ 182 and 181 [4], and on the basis of long-range ^{13}C–^{13}C couplings in a highly enriched sample, the axial carbonyl was originally assigned [4] to the low frequency signal at δ 181. A subsequent ^{13}C COSY-45 spectrum on **1** cast some doubt on this assignment [8]. Koridze and Kizas later assigned the axial carbonyl to the high frequency resonance at δ 182 on the basis of ^{187}Os couplings, since this signal has $J(^{187}$Os–C) = 90 Hz, while the signal at δ 181 has $J(^{187}$Os–C) = 113 Hz [22]. The ^{187}Os–C couplings in a number of 48-electron Os_3 clusters containing $Os(CO)_4$ groups have been measured [22–25], and for the axial carbonyls this coupling falls in the range 84–90 Hz, whilst for the equatorial carbonyls it is larger, in the range 115–123 Hz. Koridze's assignment is based on the premise that this relationship also holds for the unsaturated 46-electron cluster **1**, though we note, in caution, that $^1J(^{187}$Os–H) appears to vary according to whether the system is saturated or unsaturated [14,18]. Our results on cluster **2e**, however, bear out Koridze's assumption, since assignments of resonances a and b are unambiguous on the basis of

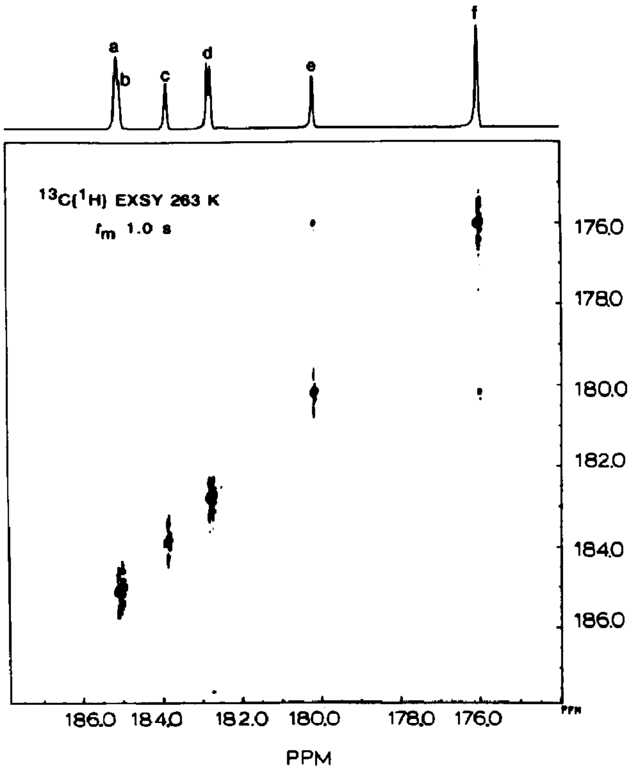

Fig. 4. ^{13}C EXSY spectrum of $Os_3(\mu\text{-}H)_2(CO)_9P^iPr_3$, **2e**, in the carbonyl region.

intensities. The assignment of the axial CO's of the $Os(CO)_4$ group in cluster **1** to the high frequency resonance must now be considered firm. Pomeroy et al. reach the same conclusion on the basis of chemical shift arguments [14].

*Fluxionality of $Os_3(\mu\text{-}H)_2(CO)_9\{P(o\text{-}tolyl)_3\}$, **2f***

Both clusters **2f** and **2g**, with bulky triarylphosphines, show no evidence for any isomer apart from 2_{eq}. The ^1H spectrum of **2f** shows complex changes with temperature in the aryl region, and a decoalescence in the methyl region, Fig. 5. A broad singlet at 298 K collapses to three singlets at 213 K. Over the same range the hydride signal collapses from a sharp doublet (δ -10.05, $J(P\text{-}H) = 6.4$) to a poorly resolved triplet. Line-shape analysis on the methyl exchange gives a value of $\Delta G^{\ddagger}_{253} = 56.5(\pm 1.2)$ kJ mol^{-1}.

The free phosphine $P(o\text{-}tolyl)_3$ has all the methyl groups equivalent in solution and the solid state structure [26] shows it adopts the "three-forward" conformation, i.e. with all three methyl groups pointing towards the P lone-pair. In mononuclear complexes it prefers to adopt the "two-forward one-back" configuration [27–31], although in uncrowded environments the "three-forward" configuration may also be observed [32]. The aryl groups in triarylphosphines generally adopt the chiral propellor configuration, and this is sometimes observed for $P(o\text{-}tolyl)_3$ in complexes [31,32], although non-propellor configurations are also observed [27–29]. In the absence of structural data on **2f**, it is difficult to draw firm conclusions from the NMR studies. The low temperature ^1H spectrum and molecular models based on the structure of the PPh_3 derivative [11] suggest that three rotomers (based on the

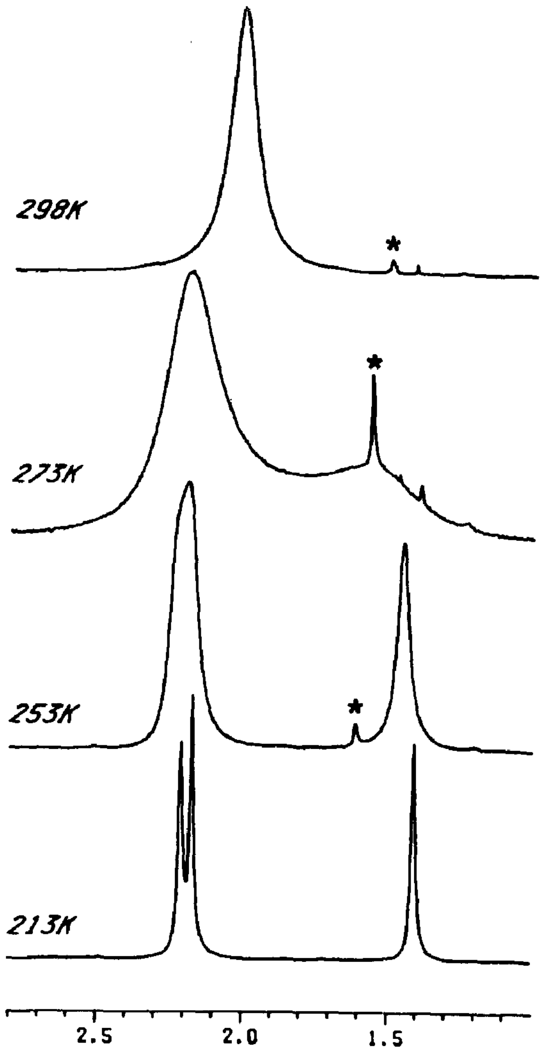

Fig. 5. ^{1}H NMR spectrum of $Os_3(\mu\text{-}H)_2(CO)_9\{P(o\text{-tolyl})_3\}$, **2f**, in the methyl region. The asterisk indicates an impurity.

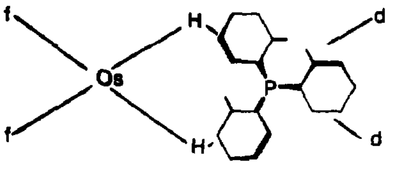

i

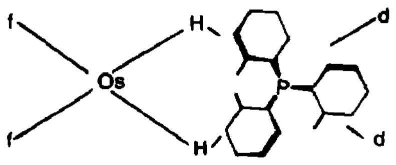

ii

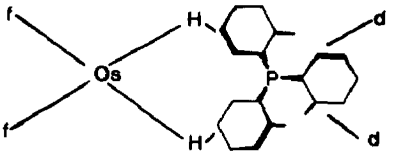

iii

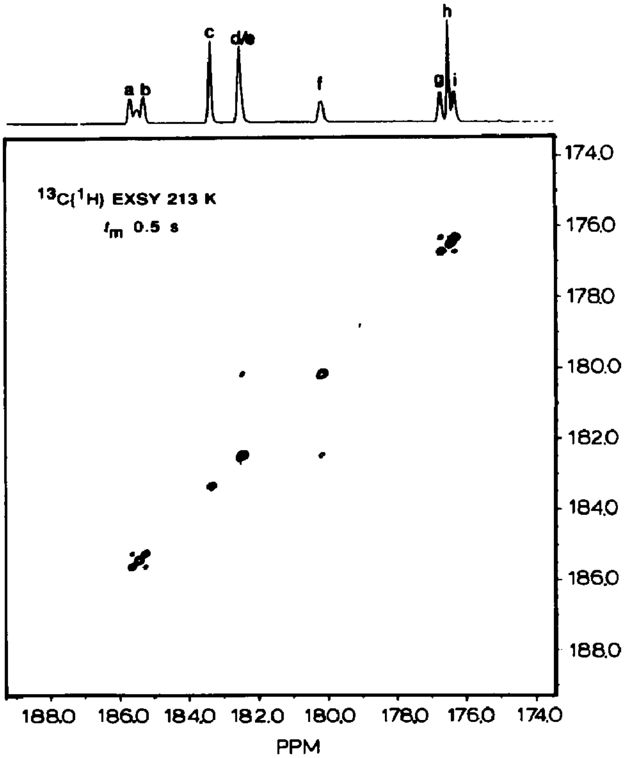

Fig. 6. ^{13}C EXSY spectrum of $Os_3(\mu\text{-}H)_2(CO)_9\{P(o\text{-tolyl})_3\}$, **2f**, in the carbonyl region.

"two-forward one-back" conformation) are possible (i), (ii) and (iii), with (i) being the most favourable. NOE studies at 213 K unfortunately proved to be inconclusive. Irradiation of the two methyl resonances at ca δ 2.2 resulted in enhancement of the hydride signal, and irradiation of this latter resonance enhanced these two Me signals and some in the aromatic region. However, the close proximity of the two Me signals at ca δ 2.2 precludes an unambiguous assignment of the conformation.

The ^{13}C spectrum at low temperatures shows nine signals for the CO ligands, indicating loss of the effective mirror plane through the Os_3 triangle. The EXSY spectrum, shown in Fig. 6, indicates pairwise exchange between resonances a and b, e and f, and g and i. From the coalescence temperature of 273 K for the e/f exchange a value of $\Delta G^{\ddagger}_{273} = 54.1(\pm 0.6)$ kJ mol^{-1} is estimated. The inequivalencies could arise either from a slowed inversion of the chirality of the propellor configuration, since the exchanging resonances represent diastereotopic carbonyls, or alternatively from a rigid single conformation. The inversion of helicity of the PR_3 ligand shown in Scheme 1 is consistent with the CO exchange, but it requires a three-ring flip for a single-stage process. The dynamic stereochemistry of organic propellors has been studied in some considerable detail [33], and in almost all cases the lowest energy process is the two-ring flip. Since the methyl environments of the phosphine undergo exchange, a three-ring flip cannot be the only dynamic process involving aryl ring flipping. The two-ring flip exchanges methyl environments, since it converts the "two-forward one-back" configuration into a "two-back one-forward", but it is a non-degenerate process and is hence likely to be of higher energy than the degenerate three-ring flip. The $\Delta G^{\ddagger}$ values obtained for the exchanges in the ^1H and

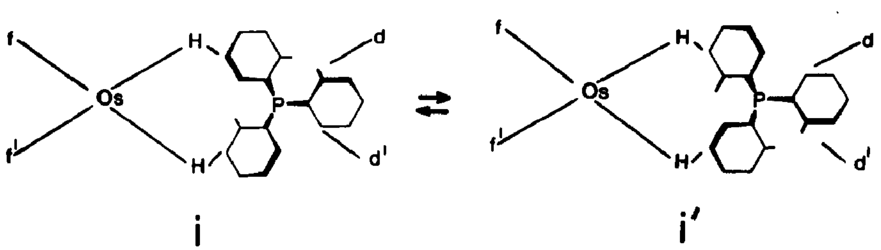

Scheme 1

^{13}C spectra suggest that separate processes are involved, although the accuracies obtained are not high. Due to the complexity of this system we have not examined the dynamics in further detail. The ^{31}P spectrum shows a singlet resonance at δ 21.5, and is invariant with temperature, which does suggest that only one conformation is populated.

Fluxionality of $Os_3(\mu\text{-}H)_2(CO)_9\{PPh(1\text{-}naphthyl)_2\}$ (2g)

For the phosphine PPh(1-naphthyl)$_2$ the three rotomers equivalent to (i) (ii) and (iii) cannot interconvert simply through aryl ring flips, since one ring is chemically different from the other two. This is evident in the low temperature ^{31}P spectrum (Fig. 7), which shows three unequally populated rotomers with $\delta(^{31}P) = 21.0$, 18.2 and 17.2 (relative ratios 3.1 : 1.6 : 10). These are in fast exchange at 298 K. The two

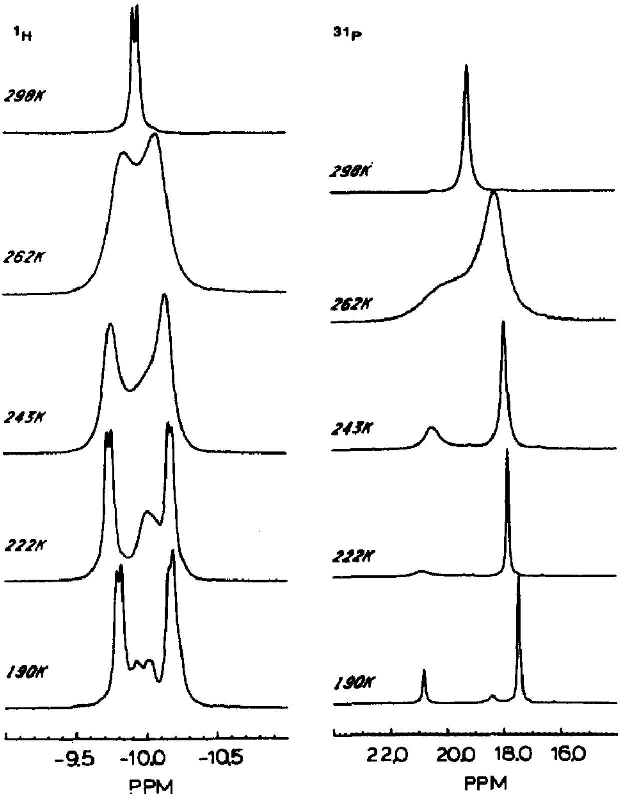

Fig. 7. ^{1}H (hydride region) and ^{31}P NMR spectra of $Os_3(\mu\text{-}H)_2(CO)_9\{PPh(1\text{-}naphthyl)_2\}$, **2g**.

Fig. 8. ^{13}C NMR spectrum of $Os_3(\mu\text{-}H)_2(CO)_9\{PPh(1\text{-naphthyl})_2\}$, **2g**, in the carbonyl region.

higher energy rotomers are in fast exchange at 222 K, and it is only above this temperature that exchange occurs with the more stable rotomer. The ^{1}H spectrum in the hydride region mirrors these effects, and in this case two distinct shifts for the chemically differing hydrides in the major rotomer are observed at δ -9.8 and -10.2. As seen for **2f**, exchange processes involving rapid rotation about the Os–P bond and helicity inversion must be responsible for the effective mirror plane through the Os_3 triangle at 298 K. The ^{13}C spectrum (Fig. 8) shows the expected pairwise collapse of resonances a/b, e/f and g/i. From the coalescence temperature of 262 K for the e/f exchange a value of $\Delta G^{\ddagger}_{262} = 51.6(\pm 0.6)$ kJ mol^{-1} is estimated for this process. At 308 K resonances g/h/i collapse into a singlet, with $J_{av}(^{187}Os\text{–}C) = 109$ Hz, showing that a tripodal rotation of the $Os(CO)_3$ group is occurring, though no estimate of the activation barrier was made.

Conclusions

The fluxionality in clusters **2** is similar to that in the unsubstituted precursor **1** [4–8], in that the only CO exchange observed involves tripodal rotation of either an $Os(CO)_3$ or $Os(CO)_2(PR_3)$ group. The former process is degenerate, and the latter non-degenerate, resulting in exchange of isomers 2_{eq} and 2_{ax}. The 2_{ax} isomer is only detected for the sterically undemanding phosphines PMe_3 and PMe_2Ph. From an EXSY spectrum on **1** at 298 K, we estimate a rate for $Os(CO)_3$ tripodal rotation of 0.64 s^{-1} using the method of Abel et al. [21], giving $\Delta G^{\ddagger}_{298} = 74.1(\pm 1.3)$ kJ mol^{-1}. The values for the same process in **2a** and **2e** are ca 4 kJ mol^{-1} lower, and this tripodal exchange is also observed with very bulky phosphines. This implies that steric factors are not important in determining the barrier to tripodal exchange.

Experimental

^{13}CO-enriched samples of clusters **2a**, **2d**, **2e**, **2f** and **2g** were prepared by a slight modification of that previously described [9]. The phosphines PMe_2Ph, PMe_3, $P(o\text{-tolyl})_3$ (Aldrich) and P^iPr_3 (Strem) were used as received; a sample of $PPh(1\text{-naphthyl})_2$ was kindly donated by Dr. R. Keat. $Os_3(\mu\text{-}H)_2(CO)_{10}$ was prepared by the literature method [34]. ^{13}CO (99% ^{13}C) was obtained from MSD Isotopes. ^1H, ^{13}C and ^{31}P NMR spectra in CD_2Cl_2 as solvent were recorded on a Bruker AM200 FT NMR spectrometer at 200.13, 50.32 and 81.0 MHz, respectively. ^1H and ^{13}C spectra were referenced to internal solvent signals and are reported relative to Me_4Si. ^{31}P spectra are referenced to 85% H_3PO_4. Phase-sensitive ^{13}C EXSY spectra were obtained using the Bruker microprogram NOESYPH and processed as previously described [18]. Rate data were obtained by the method of Abel et al. [21] using the program D2DNMR. Lineshape analysis was carried out using a locally adapted version of the program DNMR3 [35].

Preparation of ^{13}CO-enriched $Os_3(\mu\text{-}H)_2(CO)_9(PMe_2Ph)$, **2a**

To a solution of $Os_3(\mu\text{-}H)_2(CO)_{10}$ (0.3 g, 0.35 mmol) in cyclohexane (100 ml) was slowly added a solution of PMe_2Ph (0.35 mmol) in hexane until the deep-purple colour gave way to bright yellow. This solution was stirred under 1 atm ^{13}CO for ca 0.5 h, and then refluxed for 1.5 h under a nitrogen purge. The purplish solution was concentrated, and chromatographed on Florosil with hexane/dichloromethane mixtures as eluants. The purple band was collected and recrystallised from hexane to afford dark-purple crystals of $Os_3(\mu\text{-}H)_2(CO)_9(PMe_2Ph)$ (0.25 g, 85%). Enrichment levels were typically 20–40%. Samples of the other derivatives were prepared analogously, the reaction with $P(o\text{-tolyl})_3$ and $PPh(1\text{-naphthyl})_2$ requiring heating at 90 ° C for several hours.

NMR data for $Os_3(\mu\text{-}H)_2(CO)_9(PMe_2Ph)$, **2a**

^1H: (233 K) 2_{eq} isomer, δ −10.85 [d, 2H, $Os(\mu\text{-}H)Os$, $J(P\text{–}H) = 7.9$, $J(Os\text{–}H) = 48.5$, 42.3 Hz], 2.3 [d, 6H, Me, $J(P\text{–}H) = 9.8$ Hz], 2_{ax} isomer, δ −11.1 [dd, 1H, $Os(\mu\text{-}H)Os$, $J(P\text{–}H) = 6.2$, $J(H\text{–}H) = 1.0$ Hz], −11.94 [dd, 1H, $Os(\mu\text{-}H)Os$, $J(P\text{–}H) = 27.3$, $J(H\text{–}H) = 1.0$ Hz], 2.08 [d, 3H, Me, $J(P\text{–}H) = 10.5$ Hz], 2.09 [d, 3H, Me, $J(P\text{–}H) = 10.6$ Hz, 1_{eq} isomer, δ −11.14 [d, 2H, $Os(\mu\text{-}H)Os$, $J(P\text{–}H) = 1.2$ Hz], 2.35 [d, 6H, Me, $J(P\text{–}H) = 9.8$ Hz].

^{13}C: (248 K) only 2_{eq} isomer observed, δ 184.9 [d, 2C, CO_a, *J*(P–H) = 1.9 Hz], 183.9 [s, 1C, $CO_{b/c}$], 183.3 [s, 1C, $CO_{b/c}$], 181.7 [d, 2C, CO_d, *J*(P–C) = 4.5, *J*(H–C) = 2.4, 10.3 Hz], 178.7 [s, 1C, CO_e, *J*(H–C) = 2.9 Hz], 176.2 [s, 2C, CO_f, *J*(Os–C) = 107, *J*(H–C) = 2.7, 13.8 Hz].

^{31}P: (244 K), 2_{eq} isomer, δ −8.3 [s, *J*(Os–P) = 193 Hz], 2_{ax} isomer, δ −17.1, 1_{eq} isomer, δ −35.7.

NMR data for $Os_3(\mu\text{-}H)_2(CO)_9(PMe_3)$, **2d**

^{1}H: (234 K) isomer 2_{eq}, δ −11.0 [d, 2H, Os(μ-H)Os, *J*(P–H) = 8.1, *J*(Os–H) = 48.6, 42.1 Hz], 1.95 [d, 9H, Me, *J*(P–H) = 10.2 Hz], isomer 2_{ax}, δ −11.20 [dd, 1H, Os(μ-H)Os, *J*(P–H) = 6.3, *J*(H–H) = 0.6 Hz], −11.69 [dd, 1H, Os(μ-H)Os, *J*(P–H) = 25.9, *J*(H–H) = 0.6 Hz], 1.80 [d, 9H, Me, *J*(P–H) = 10.8 Hz].

^{13}C: (234 K) isomer 2_{eq}, δ 185.6 [s, 2C, CO_a], 184.9 [s, 1C, $CO_{b/c}$], 184.3 [s, 1C, $CO_{b/c}$], 182.3 [d, 2C, CO_d, *J*(P–C) = 4.6 Hz], 179.2 [s, 1C, CO_e], 176.6 [s, 2C, CO_f], isomer 2_{ax}, δ 187.5, 183.4, 181.1, 181.0, 179.7, 179.6, 178.3, 178.2, 174.2.

^{31}P: (234 K) isomer 2_{eq}, δ −15.1 [s, *J*(Os–P) = 192.3 Hz], isomer 2_{ax}, δ −22.5.

NMR data for $Os_3(\mu\text{-}H)_2(CO)_9(P^iPr_3)$, **2e**

^{1}H: (298 K) isomer 2_{eq}, δ −10.92 [d, 2H, Os(μ-H)Os, *J*(P–H) = 6.6, *J*(Os–H) = 48.6, 42.0 Hz] 1.32 [dd, 18H, Me, *J*(H–H) and *J*(P–H) = 14.5, 7.1 Hz], 2.55 [m, 3H, CH], isomer 1_{eq}, δ −11.20 [d, *J*(P–H) = 7.0].

^{13}C: (298 K) δ 185.0 [d, 2C, CO_a, *J*(P–C) = 2.0, *J*(Os–C) = 92 Hz], 184.6 [s, 1C, $CO_{b/c}$, *J*(Os–C) = 116 Hz], 183.5 [s, 1C, $CO_{b/c}$], 182.5 [d, 2C, CO_d, *J*(P–C) = 4.0, *J*(Os–C) = 116, *J*(H–C) = 2.7, 9.9 Hz], 180.0 [s, 1C, CO_e, *J*(Os–C) = 113, *J*(H–C) = 3.1 Hz], 175.8 [s, 2C, CO_f, *J*(Os–C) = 107, *J*(H–C) = 2.7, 14.1 Hz].

^{31}P: (298 K) isomer 2_{eq}, δ 55.9 [s, *J*(Os–P) = 191 Hz], isomer 1_{eq}, δ 42.8.

NMR data for $Os_3(\mu\text{-}H)_2(CO)_9\{P(o\text{-}tolyl)_3\}$, **2f**

^{1}H: (298 K) δ −10.05 [d, 2H, Os(μ-H)Os, *J*(P–H) = 6.4, *J*(Os–H) = 47.6, 42.8 Hz], 2.05 [s, br, 9H, Me]; (213 K) δ −10.15 [t, br, 2H], 1.40 [s, 3H, Me], 2.15 [s, 3H, Me], 2.23 [s, 3H, Me].

^{13}C: (213 K) δ 185.6 [s, 1C, $CO_{a/a'}$, *J*(C_a–$C_{a'}$) = 33 Hz (from AB spectrum of ^{13}C–^{13}C isotopomer], 185.2 [s, 1C, $CO_{a/a'}$], 183.3 [s, 1C, $CO_{b/c}$], 182.5 [s, 2C, $CO_{b/c}$ and $CO_{d/d'}$], 180.0 [s, br, 1C, $CO_{d/d'}$], 176.7 [s, 1C, $CO_{f/f'}$], 176.5 [s, 1C, CO_e], 176.3 [s, 1C, $CO_{f/f'}$]; (308 K, toluene-d_8) δ 185.0 [s, 2C, CO_a, *J*(Os–C) = 91 Hz], 182.6 [s, 1C, $CO_{b/c}$, *J*(Os–C) = 116 Hz], 181.8 [s, 1C, $CO_{b/c}$], 180.7 [s, br, 2C, CO_d], 176.1 [s, 3C, CO_e and CO_f, J_{av}(Os–C) = 105 Hz].

^{31}P: (298 K) δ 21.4 [s, *J*(Os–P) = 197 Hz].

NMR data for $Os_3(\mu\text{-}H)_2(CO)_9\{PPh(1\text{-}naphthyl)_2\}$, **2g**

^{1}H: (298 K) δ −9.85 [d, 2H, Os(μ-H)Os, *J*(P–H) = 6.7, *J*(Os–H) = 48.2, 43.4 Hz]; (190 K) δ −9.79 (d, *J*(P–H) = 6.3 Hz), −9.9 (br), −10.0 (br), −10.15 [d, *J*(P–H) = 6.0 Hz].

^{13}C: (298 K) δ 184.9 [d, 2C, CO_a, *J*(P–C) = 1.8, *J*(Os–C) = 94 Hz], 182.8 [s, 1C, $CO_{b/c}$, *J*(Os–C) = 116 Hz], 182.0 [d, 1C, $CO_{b/c}$, *J*(Os–C) = 115 Hz], 181.0 [d, 2C, CO_d, *J*(P–C) = 3.4, *J*(Os–C) = 114, *J*(H–C) = 10.5 Hz], 176.3 [s, 1C, CO_e, *J*(Os–C) = 102, *J*(H–C) = 3 Hz], 176.1 [s, 2C, CO_f, *J*(Os–C) = 107, *J*(H–C) = 2.8, 13.8 Hz]; (222 K) δ 185.4 [s, 1C, $CO_{a/a'}$], 184.5 [s, 1C, $CO_{a/a'}$], 183.1 [s, 1C, $CO_{b/c}$], 182.3 [s, 2C, $CO_{b/c}$ and CO_d], 179.8 [2, 1C, $CO_{d'}$], 176.5 [s, 1C, $CO_{f/f'}$], 176.1 [s, 1C, CO_e], 175.5 [s, 1C, $CO_{f/f'}$].

^{31}P: (298 K) δ 20.1 [s, J(Os–P) = 200 Hz]; (190 KI) δ 21.0 [s, J(Os–P) = 199 Hz], 18.2 [s, br], 17.2 [s, J(Os–P) = 196 Hz]

X-ray structure determination

Crystal data. $C_{18}H_{23}O_9Os_3P$, $M = 984.95$, monoclinic, space group $P2_1/c$, a 15.762(7), b 11.143(3), c 16.398(7) Å, $\beta = 118.15(3)°$, V 2539(2) Å^3, $Z = 4$, D_c 2.58 g cm^{-1}, $F(000) = 1784$, μ(Mo-K_α) = 151.0 cm^{-1}.

A crystal of approximate dimensions 0.25 × 0.55 × 0.7 mm was mounted in a general position on a glass fibre and coated with acrylic resin. Data were collected at ambient temperatures, using the $\theta/2\theta$ scan mode, on a CAD4F automated diffractometer with graphite monochromated X-radiation (λ = 0.71069 Å). Unit cell parameters were determined by refinement of the setting angles ($\theta \geqslant 12°$) of 25 reflections. The standard reflections 262 and $9\bar{3}\bar{4}$ were measured every 2 h and no significant decay in intensities was observed. Lorentz-polarisation and absorption/extinction (DIFABS [36]) corrections were also applied. A total of 2647 measured reflections (θ range 2–20°, h $0 \rightarrow 15$, k $0 \rightarrow 10$, l $-15 \rightarrow +15$) yielded 2364 independent data, of which 1819 having an intensity $> 3\sigma(I)$ were considered observed and used for structure solution and refinement. Systematic absences uniquely determine the centrosymmetric space group $P2_1/c$. The structure was solved by direct methods (MITHRIL [37]) and subsequent electron density difference syntheses. Refinement was by full-matrix least-squares minimising the function $\Sigma w(|F_o| - |F_c|)^2$ with the weighting scheme $w = [\sigma^2(F_o)]^{-1}$ used and judged satisfactory. $\sigma(F_o)$ was estimated from counting statistics. Alkyl hydrogen atoms (C–H = 1.0 Å), and hydrides (HYDEX [38], Os–H ~ 1.85 Å) were included at calculated positions, with fixed contributions to the structure factors. Refinement using a total of 145 parameters converged at $R(R_w) = 0.038(0.043)$, with mean and maximum Δ/σ values of 0.007 and 0.03, respectively, in the final cycle. A final electron density difference synthesis showed no chemically significant features (max $\Delta\rho = +0.86$, min $\Delta\rho = -1.07$ e Å^{-3}). The esd of an observation of unit weight (S) was 1.77. Neutral atom scattering factors were taken from reference 39 with corrections applied for anomalous scattering. All calculations were carried out on a Micro-VAX 3600 computer using the Glasgow GX suite of programs [40].

Supplementary material. Lists of observed and calculated structure factors, thermal parameters, and a complete listing of bond lengths and angles are available from the author.

Acknowledgement

Johnson-Matthey is thanked for a generous loan of OsO_4.

References

1 E. Band and E.L. Muetterties, Chem. Rev., 78 (1978) 639.
2 B.F.G. Johnson and R.E. Benfield, in B.F.G Johnson (Ed.), Transition Metal Clusters, Wiley, Chichester, 1980.

3 J.B. Keister and J.R. Shapley, Inorg. Chem., 21 (1982) 3304.
4 S. Aime, Inorg. Chim. Acta, 62 (1982) 51.
5 S. Aime, D. Osella, L. Milone and E. Rosenberg, J. Organomet. Chem., 213 (1981) 207.
6 E. Rosenberg, E.V. Anslyn, C. Barner-Thorsen, S. Aime, D. Osella, R. Gobetto and L. Milone, Organometallics, 3 (1984) 1790.
7 G.E. Hawkes, E.W. Randall, S. Aime, D. Osella and J.E. Elliot, J. Chem. Soc., Dalton Trans., (1984) 279.
8 G.E. Hawkes, L.Y. Lian, E.W. Randall, K.D. Sales and S. Aime, J. Chem. Soc., Dalton Trans., (1985) 225.
9 A.J. Deeming and S. Hasso, J. Organomet. Chem., 114 (1976) 313.
10 E.G. Bryan, W.G. Jackson, B.F.G. Johnson, J.W. Kelland, J. Lewis and K.T. Schorpp, J. Organomet. Chem., 108 (9176) 385.
11 R.E. Benfield, B.F.G. Johnson, J. Lewis, P.R. Raithby, C. Zuccaro and K. Hendrick, Acta Crystallogr., Sect. B., B35 (1979) 2210.
12 R.D. Adams and B.E. Segmüller, Cryst. Struct. Commun., 11 (1982) 1971.
13 (a) R.D. Adams and N.M. Golembeski, Inorg. Chem., 18 (1979) 1909; (b) R.D. Adams and N.M. Golembeski, J. Am. Chem. Soc., 101 (1979) 2579.
14 A.K. Ma, F.W.B. Einstein, V.J. Johnston and R.K. Pomeroy, Organometallics, 9 (1990) 45.
15 M.R. Churchill, F.J. Hollander and J.P. Hutchinson, Inorg. Chem., 16 (1977) 2697.
16 C.A. Tolman, Chem. Rev., 77 (1977) 313.
17 E. Rosenberg, C. Barner-Thorsen, L. Milone and S. Aime, Inorg. Chem., 24 (1985) 231.
18 L.J. Farrugia, Organometallics, 8 (1989) 2410.
19 A.J. Deeming, S. Donovan-Mtunzi, S.E. Kabir and P.J. Manning, J. Chem. Soc., Dalton Trans., (1985) 1037.
20 R. Willem, Prog. Nucl. Magn. Reson. Spectrosc., 20 (1988) 1.
21 E.W. Abel, T.P.J. Coston, K.G. Orrell, V. Sik and D. Stephenson, J. Magn. Reson., 70 (1986) 34.
22 A.A. Koridze and O.A. Kizas, Metallorg. Khim., 2 (1989) 177 [English translation; Organomet. Chem. USSR, 2 (1989) 87].
23 A.A. Koridze, O.A. Kizas, N.M. Astakhova, P.V. Petrovskii and Yu.K. Grishin, J. Chem. Soc., Chem. Commun., (1981) 853.
24 M.A. Gallop, B.F.G. Johnson and J. Lewis, J. Chem. Soc., Chem. Commun., (1987) 1831.
25 P. Ewing, L.J. Farrugia and D.S. Rycroft, Organometallics, 7 (1988) 859.
26 T.S. Cameron and B. Dahlen, J. Chem. Soc., Perkin Trans. 2, (1975) 1737.
27 S. Okeya, T. Miyamoto, S. Ooi, Y. Nakamura and S. Kawaguchi, Bull. Chem. Soc. Jpn., 57 (1984) 395.
28 S. Ooi, T. Matsushita, K. Nishimoto, S. Okeya, Y. Nakamura and S. Kawaguchi, Bull. Chem. Soc. Jpn., 56 (1983) 3297.
29 E.C. Alyea, S.A. Dias, G. Ferguson, M.A. Khan and P.J. Roberts, Inorg. Chem., 18 (1979) 2433.
30 E.C. Alyea, S.A. Dias, G. Ferguson and P.J. Roberts, J. Chem. Soc., Dalton Trans., (1979) 948.
31 R. Brady, W.H. De Camp, B.R. Flynn, M.L. Schneider, J.D. Scott, L. Vaska and M.F.W. Erneke, Inorg. Chem., 14 (1975) 2669.
32 E.C. Alyea, S.A. Dias, G. Ferguson and M. Khan, Can. J. Chem., 57 (1979) 2217.
33 J. Brocas, M. Gielen and R. Willem (Eds.), The Permutational Approach to Dynamical Stereochemistry, McGraw-Hill, New York, 1983, Ch. 13.
34 S.A.R. Knox, J.W. Koepke, M.A. Andrews and H.D. Kaesz, J. Am. Chem. Soc., 97 (1975) 3942.
35 D.A. Kleier and G. Binsch, QCPE, 11 (1970) 165.
36 N. Walker and D. Stuart, Acta. Crystallogr., Sect. A., Found Crystallogr., A39 (1983) 158.
37 C.J. Gilmore, J. Appl. Crystallogr., 17 (1984) 42.
38 A.G. Orpen, J. Chem. Soc., Dalton Trans., (1980) 2509.
39 International Tables for X-Ray Crystallography, Kynoch Press, Birmingham, 1974, Vol. 4.
40 P.R. Mallinson and K.W. Muir, J. Appl. Crystallogr., 18 (1985) 51.